The Hume-Rothery size rule and double-well microstructures in gold-nickel

2001 J. Phys.: Condens. Matter 13 8661

(http://iopscience.iop.org/0953-8984/13/38/309)

INSTITUTE OF PHYSICS PUBLISHING JOURNAL OF PHYSICS: CONDENSED MATTER

J. Phys.: Condens. Matter **13** (2001) 8661–8676 PII: S0953-8984(01)24857-7

The Hume-Rothery size rule and double-well microstructures in gold–nickel

K Janghorban[1,2], J S Kirkaldy[2] and G C Weatherly[2]

[1] Materials Science Department, Shiraz University, Iran
[2] Brockhouse Institute for Materials Research, McMaster University, Hamilton, Canada L8S 4M1

Received 16 May 2001
Published 7 September 2001
Online at stacks.iop.org/JPhysCM/13/8661

Abstract

The miscibility gap and high critical temperature in Au–Ni together with coherency strain effects in decomposition arise primarily due to the Pauli principle, whereby the fcc lattice parameter of Au is 1.15 times that of Ni, thus acting maximally according to Hume-Rothery against extensive solid solution formation. Since the critical point is only about 100 °C below the solidus, this simplifies the theoretical evaluation of the solubility limitation. It also offers a bridge to spinodal kinetics encompassing a *dominant solution effect* of local Vegard's law strain, which acts repulsively in bulk clustering and attractively in gradient energy relaxation. Low and high temperature TEM hot stage observations of continuous modulated decomposition spanning the miscibility gap of Au–Ni ($T_c \simeq 1080$ K) can be interpreted according to the time-dependent Ginzburg–Landau (TDGL) reaction–diffusion theory modified to include solute conservation and a diffusion-relaxable effect of strain while maintaining full low amplitude coherency. Modulated decomposition structures of order 3 nm, proven through lattice imaging to be spinodal in character by Sinclair *et al*, have often been reported near the so-called upper limit, coherent critical temperature (∼420 K), where the wavelength is supposed to be infinite, while we report here well advanced 10 nm modulations at 350 °C above this. As a crystallographic template, the fine three-dimensional interleaved dendrite-like tweed pattern first decoheres, then locally transforms at 773 K into ∼100 nm lamellar spacing intragranular nodules. These coarsened bulk products are modulation-templated, faceted, near-spherical structures, first observed by Underwood between 673 and 973 K and by Cahn at 993 K in 1954, and prove to be consistent with steady state lamellar solutions of the TDGL equation. This three-stage decomposition mode in ∼100 nm thick films competes with the well known grain-boundary-nucleated short-circuited lamellar product, which was originally deemed to be unique in bulk samples at higher temperatures.

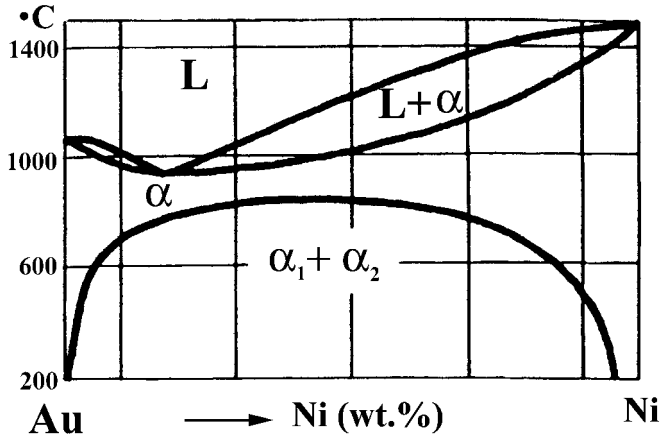

Figure 1. The Au–Ni phase diagram exhibiting the miscibility gap [3].

1. Introduction

Pearson [1] summarizes the empirical size rule of Hume-Rothery with the statement that 'unless the solute and solvent radii fall within about 15% of each other extensive solid solutions cannot be formed even though all other factors are favourable. As this rule holds generally it can be predicted with some certainty that extensive solid solutions will *not* form in any system where the radii differ by more than 15%'. The existence of such a well established empirical rule is proof that the relative size effect is a unique contribution to solution thermodynamics in the usual sense of excess unlike atomic repulsion or attraction. This exists in a stochastic vacancy-moderated self-diffusing milieu with barrier-mounting chemical free energies of $kT/2$ per atom per degree of freedom, which approaches the pairing energy density [2]. This phase diagram limitation, which anticipates a clustering transformation, can be derived in solid state alloy solution theory via the establishment of a transitive relation ($\leqslant$) between the strain energy density and the approximate total pair energy density $2n_v kT_c$. With the fcc lattice parameter ratio of Au/Ni of 1.15 it is evident that the rule is exhibited at the equality margin of this criterion where, since T_c approaches the solidus temperature (compare the phase diagram of figure 1 [3]), the strain energy density represents close to the total pair energy density. Pearson [1] and Friedel [4] have accordingly emphasized that in general the size effect, reflecting the Pauli principle, is *primary* in the determination of the solution chemistry and therefore the detail of the miscibility gap. They note that valency differences and polarization effects also play a part, recognizing that these further electronic effects are not strictly independent.

The present article is concerned with the empirical and theoretical consequences in *kinetics* of this important contribution of Hume-Rothery, and will have much to do with understanding the sequence of modulated 773 K TEM hot stage patterns of figures 2–4. The viewing of such developing patterns *in situ* establishes from the start that we are dealing with an isothermal, strictly autonomous system, which is to say that the boundary conditions are irrelevant [5]. The heterogeneity of the pattern demands a variational approach to the theory and establishes the time-dependent Ginzburg–Landau (TDGL) reaction–diffusion equation [5–7] with a solute-conserving Lagrange multiplier as appropriate since fluctuations are the natural, quench-induced initial condition. This equation uniquely generates the Helmholz free energy as a Lyapunov functional without reference to boundary conditions [5].

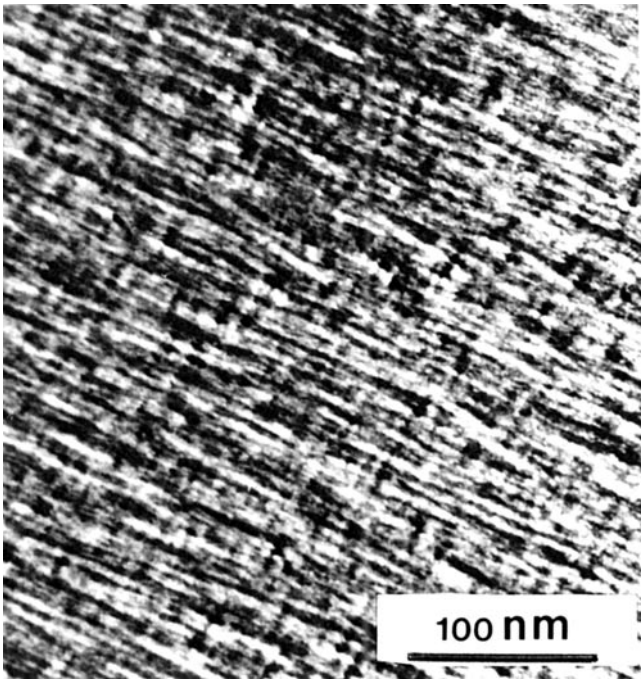

Figure 2. Spinodal modulations in Au–50 at.% Ni. 30 minutes at 773 K on the TEM hot stage.

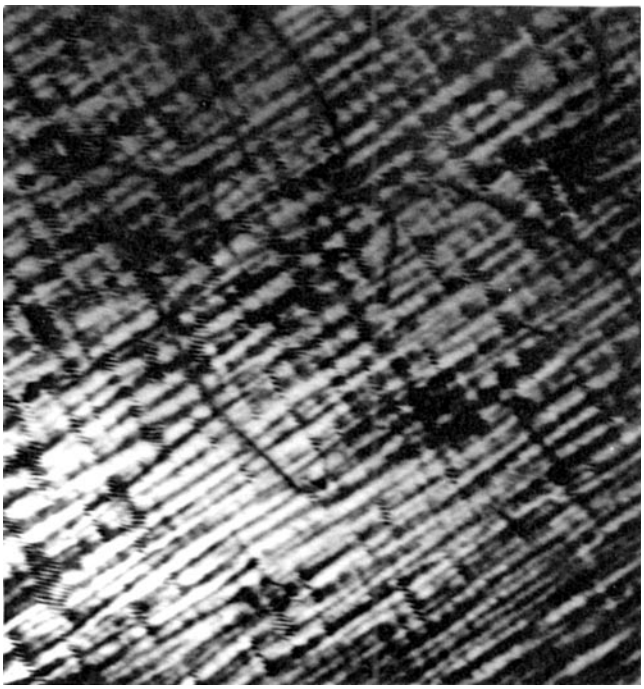

Figure 3. Spinodal modulations in Au–50 at.% Ni. 45 minutes at 773 K. Note threading dislocations, and Moiré patterns, which designate the beginning of decoherency.

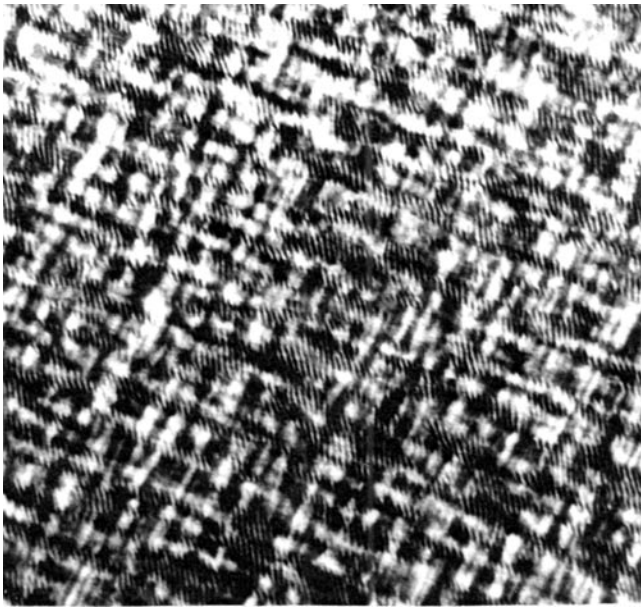

Figure 4. Spinodal modulations in Au–50 at.% Ni. 60 minutes at 773 K. A more advanced stage of decoherency.

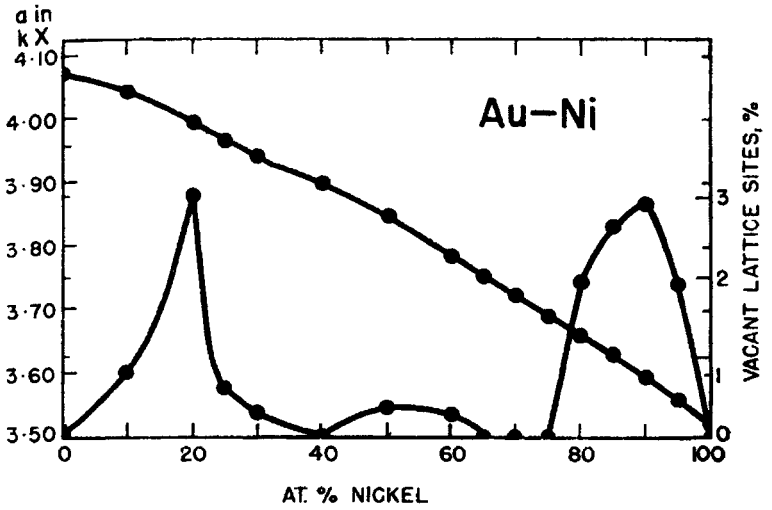

Figure 5. Lattice spacing and percentage vacant lattice sites of the Au–Ni solid solution as a function of composition [1].

The foregoing Au–Ni results are consistent with the near-linearity of the lattice parameter in figure 5 [1], which approaches Vegard's law and can be extended to address the kinetics. We argue from the aforementioned direct relationship due to Friedel [4] that the strain energy density is a repulsive electronic pairing effect [8, 9] so must combine as a responsively attractive downhill diffusion effect with valency and/or polarization contributions to the effective pair energy density as they appear within the gradient energy coefficient. This coupling is presumed

to occur without causing loss of coherence. This is in contrast with the more elaborate Cahn–Hilliard diffusion theory [10], which disallows both a naturally fluctuating initial condition and diffusion relaxation of strain energy. It is likely that both viewpoints represent polar extremes of a more general theory yet to be worked out, a matter which we will address at the end.

The slight lattice parameter curvature in figure 5 [1] can reasonably be attributed to the known augmentation of the nickel valency (2 or 3) relative to that of Au (1 or 2). Such an eventuality is undoubtedly at the root of the much-augmented vacancy densities recorded in figure 5. Because its sign represents lattice expansion, decomposition of an alloy means creation of free volume, which can abet decoherency at sufficient amplitudes. This sign is the opposite of that implied by the Cahn–Hilliard coherency effect, which by ignoring fluctuations and invoking strain energy relaxation, collapses the alloyed lattice into an ostensibly more stable configuration at the higher temperatures.

In a related empirical investigation of $L1_2$ ordering of the form Ni_3X Pearson [11] has concluded that this phase formation is denied by the Hume-Rothery size effect if $r_X > 1.12r_{Ni}$ thus excluding its equilibrium appearance in Au–Ni alloys. Notwithstanding, $L1_2$ satellites in TEM observations on transforming Au–Ni alloys between 25 and 75% at 773 K have been observed (figure 6). We shall argue in a separate contribution that this is a purely dynamical consequence of the accompanying modulation formations.

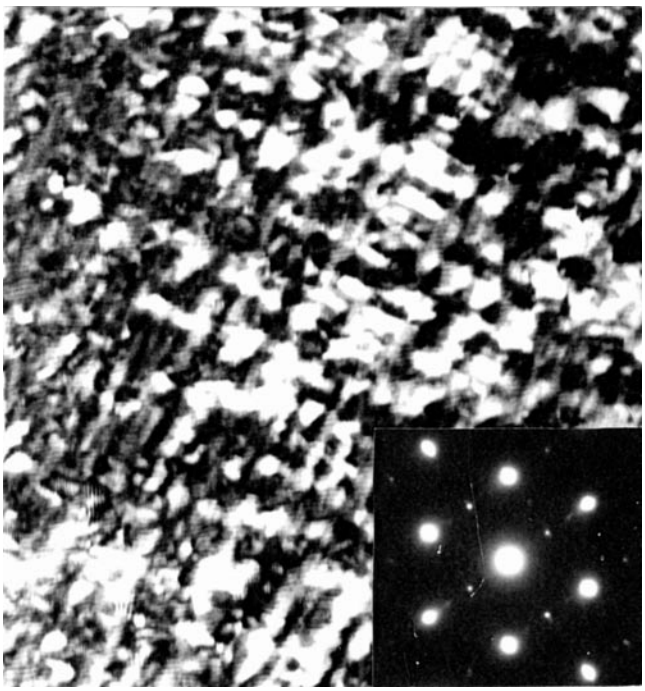

Figure 6. Continuation of the series 2–4 to 90 minutes. Appearance of Ni_3Au superlattice satellites.

Figure 7 exhibits the miscibility gap of Au–Ni as proposed by Abadias *et al* [12]. This superimposes the currently predicted effect of coherency plane strain on the critical point and spinodal line according to the long range strain-dependent fourth order diffusion theory [10]. These authors have identified in the figure a compendium of recorded modulation observations such as in figure 3 by their composition and quench temperature and these exhibit wavelengths of 1 to 5 nm, the range presumably reflecting composition and different thermal paths taken

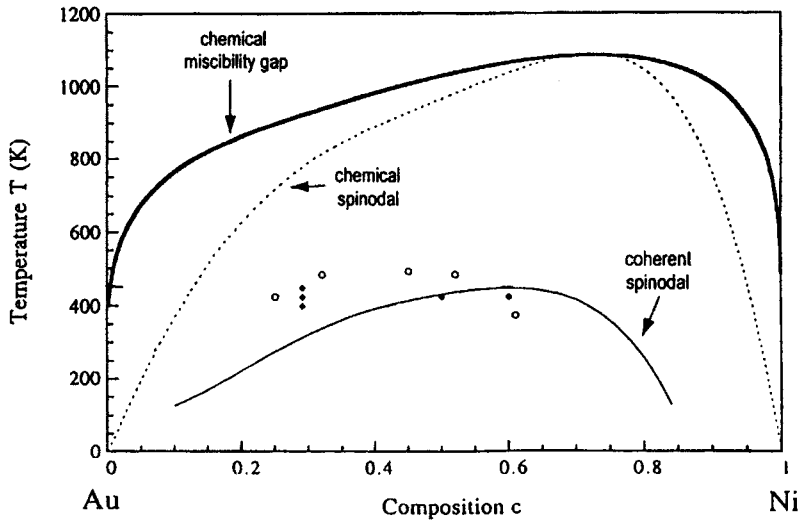

Figure 7. Phase diagrams of the Au–Ni system: chemical miscibility gap (bold line), chemical spinodal (dashed line) calculated from Cook and Hilliard's method and calculated coherent spinodal (solid curve). Some experimental values (○) and (◆) are also reported.

to reach the decomposition isotherm. Since in Cahn–Hilliard theory the coherent critical temperature T_{cc} defines an infinite cut-off wavelength we have taken these short wavelength observations as notice of a potential discrepancy, discounting the proposition that TEM thin film surfaces offer a three-dimensional relaxant of coherency strain which consistently reduces the observable wavelength via distorted strain contrast to near atomic dimensions. We further note the research of Sinclair *et al* [13] on the lattice imaging of bulk decomposition in Au–Ni at 423 K, which clearly identifies 3 nm strain modulations in subsequently thinned specimens of expected Vegard's law misfit magnitude.

Early investigations on bulk polycrystalline alloys, primarily involving light microscopy and x-ray lattice parameter measurements [14–16], focused upon the higher temperatures (>600 K), where a grain boundary nucleated lamellar reaction product seemed to dominate, and this has been commonly identified with the terminal solution process of discontinuous precipitation [17]. This reaction involves one product phase with its composition stepped discontinuously from the mother phase and proceeding via frontal boundary short circuit diffusion. However, Au–Ni differs from the norm for that process in the observation that the two lamellar reaction products closely approach the equilibrium concentrations without a non-equilibrium step [14, 16], being as normally implied by the phase diagram. More significant is Underwood's observation of frequent intracrystalline near-spherical faceted lamellar nodules [15], which we have confirmed (figure 8). The cube faceting and near spherical reaction fronts suggest that there must have been a nucleate coarsening step which is crystallographically defined. This turned out to be the spinodal cube–cube modulations themselves, which undergo a complex coarsening reaction while maintaining a near single crystal disposition. The lamellar reaction as a steady state *single crystal* process in Au–Ni had been predicted by one of us on the grounds that the TDGL equation possesses an appropriate two-dimensional solution for steady state lamellar spinodal decomposition [18, 19]. Current observations, summarized in the following section, provide firm microscopic evidence that the increased scale of the tertiary lamellar coarsened reaction is crystallographically templated by the fine continuous

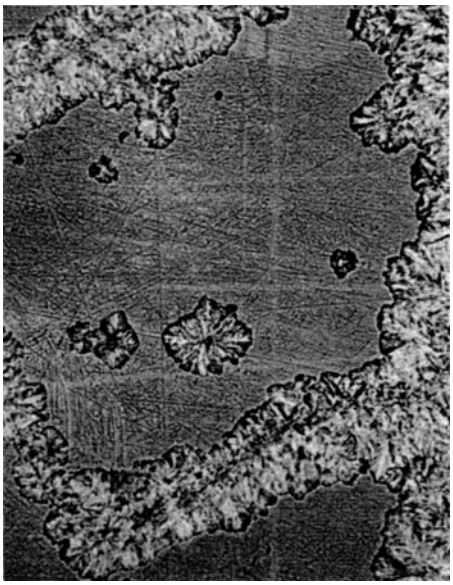

Figure 8. Cross-sections of dendritic lamellar nodules in Au–38 at.% Ni at 673 K exhibiting faceting in cube directions. Note the faceting of the three largest nodules in comparison with the deduced nucleation events (figure 10), implying common templating lattice modulations undergoing coarsening. The largest nodule is 10 μm in diameter.

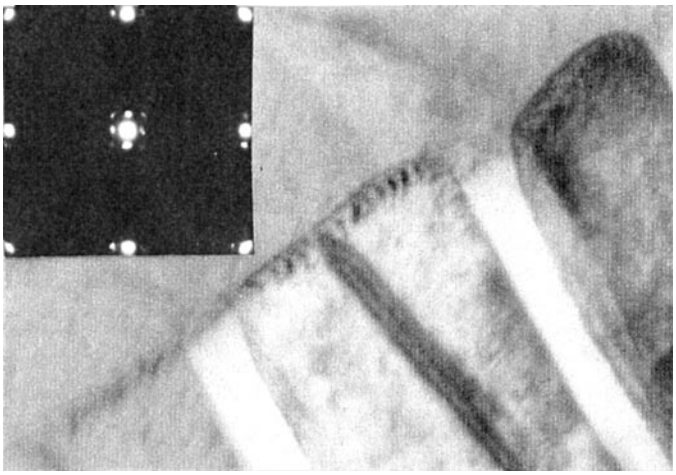

Figure 9. Representative lamellar front in Au–38% Ni at 673 K. The electron diffraction inset establishes the cube–cube relationship between lamellar product phases. Note the frontal misfit dislocations. Spacing approximately 0.1 μm.

modulations in two or three dimensions. Since the coarsening process is deeply intragranular, the precursor high strain energy density upon decohering and conversion *must* contribute to the rich source of dislocations which ultimately makes up the highly conducting lamellar phase boundary (figure 9).

In the later theoretical sections we will undertake the explanation of the following observations within the scope of the second order TDGL reaction–diffusion equation in

which the locally strain-induced repulsive clustering term subsumes a vacancy-moderated, fluctuation-initiated homogeneous reaction subject to the opposing Le Chatelier response and contribution upon loss of coherency to a gradient energy driven reversion process. This approach will be contrasted with the conventional fourth order theory in various versions, which, relying upon quasi-static arguments, generates a number of paradoxes.

2. TEM hot stage experiments at 773 K

In planning the present key experiments the sometimes artifact-prone character of previous TEM observations was examined. Some of these earlier experiments were repeated over a range of temperatures and compositions (cf figure 8) and these as well as figure 9 verified a universal cube–cube relation between the two coarse lamellar product phases despite their necessary lack of a unique habit plane in the often dendrite-like, near-spherical colonies. Notwithstanding this lack of perfect organization, the nodules exhibited frontal facets which point towards a mother–product orientation relation and therefore a near single crystal reaction, evidently inherited from the initiating three-dimensional modulations. Ultimately a range of alloys at 773 K were chosen together with TEM *in situ* hot stage observations in the 100 nm thick portion of thin films as to be the most likely to offer transparent bulk behaviour and theoretical significance. Such a film thickness avoids the very thin edge artifacts including copious unwanted dislocation generation, minimizes surface relaxation effects relative to the total strain energy in 10 or 15 nm modulations, offers sufficient strain contrast for observing modulations and misfit dislocations and limits the probability of early interference in the film by rich grain boundary originated lamellar products normally in profusion in the bulk. Four compositions were examined on the TEM hot stage: 25, 38, 50 and 75 at.% Ni for periods from 10 to 90 min.

As well as composition modulations, superlattice satellites of Ni_3Au were detected in all cases (figure 6). While the presence of this local long range ordering mode might suggest the presence of a previously undetected metastable line compound, it is our view based upon Pearson's Ni_3X survey [11] within the Hume-Rothery atom size paradigm, that the ordering is probably a purely dynamical effect of the class described by Krznowski and Allen [20], Chen and Khachaturyan [21] and by Maugis [22]. This can also be rationalized more generally in terms of Ostwald's step rule requiring reactive path selection through the highest possible free energy states.

The typical sequence of figures 2–4 and 6 represents the precursors of the colonies seen in figure 8. Careful examination of the contrast in a 100 nm thick sample implies that the spinodal structure consists of an interleaved pair of imperfect three-dimensional dendrites, one solute rich and the other solute poor and separated by an array of connected incipient saddle surfaces. Within this representation the internal stresses and associated strains of whatever origin are of a capillary or gradient energy disposition. Already in figure 3 the intragranular pattern amplitude with its cumulative strain energy has begun to decohere as evidenced by the Moiré fringes. This instability could have been catalysed by the free surface, but this is not essential since with linear amplitude increase, excess free volume has been quadratically produced (figure 5), contributing in bulk to a threshold for activation and folding of the threading dislocations present. While we have not directly observed the full role played by dislocations in the subsequent coarsening reaction, circumstantially they must be created by dissipative combination of free volume and excess strain energy and coherently rearranged to accommodate composition reversion and provide a frontal conducting surface for the intragranular lamellar products of figure 8. We have, however, observed the intermediate change in microstructure as recorded *in situ* in figure 10. The emerging coarse dendritic form (figure 11) is in very good {100} correspondence

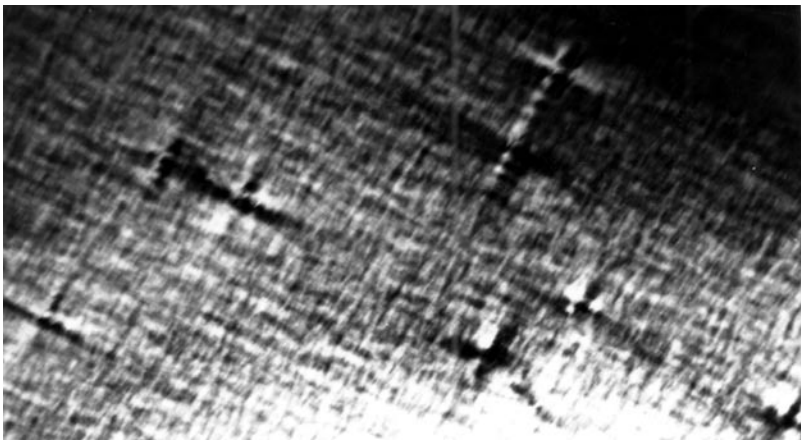

Figure 10. Successor to figure 3 indicating local pre-coarsening instability, which acts as the template nucleus for the dendrite cores of figures 11 and 12. See figure 2 for scale.

Figure 11. Directional [100] dendrite with bainite-like two-phase lamellar side-branches coarsened from the modulation instabilities of figure 10 evolving into the nodules of figures 12 and 8. See figure 2 for scale of modulations.

with the single crystal substrate and the initiating remnant of the coherent modulations as the attached diffraction patterns prove. This manifestation may be designated as the 'nucleus' of the faceted near-spherical colonies (figures 8 and 12) which evolve from it. Despite the lack of defined habit planes in the colonies the two product phases remain in a cube–cube relationship together with a cube relationship of the dendritic cores to the mother structure (figure 8). We are accordingly justified in designating the coarse lamellar product as a near steady state spinodal decomposition.

This last thin film observation of figure 12 is extremely important in the validation of the experimental interpretation including the uniqueness of a theoretical kinetic format. Firstly, it

Figure 12. Near lamellar nodules exhibiting cube–cube branching with cube templating by the initiating modulation. Note that the two main dendrite cores to the right and left are aligned with the remnant modulations and their nucleate instabilities (figure 10). Lamellar spacing approximately 0.1 μm.

has reproduced in time-dependent detail the key results of figure 8, which had only previously been observed in bulk material. Secondly, via the dense Moiré patterns evident at higher magnification (e.g. figure 4) it has identified the source of intragranular dislocations which must be made available for constructing a lamellar frontal conducting boundary. The dominant source must be the combination of excess free volume and coherency strain energy since the outcome is the same in bulk as deduced from thin film TEM. We note, however, that the production of nodules in the bulk suffers less distortion than in thin films where surface perturbations may be expected. Finally in identifying a near single crystal lamellar mode it identifies the process with a steady state TDGL solution [18]. This necessarily brings our explanations further into conflict with the long standing fourth order diffusion equation and its coherency strain phenomenology, matters now to be discussed in greater detail. In this, one can focus on Cahn's 1961 statement that 'nothing which could possibly be interpreted as spinodal decomposition has been reported at high temperatures for Au–Ni' and the 40 year accumulation of data which has ultimately eliminated this gap in our knowledge.

3. Solute conservation in the mean field kinetic formulations of Cahn–Hilliard and Ginzburg–Landau for a 50–50 alloy

Through a general misunderstanding of the intimate connection between the symmetries of variational Lagrangians and conserving currents [23] Ginzburg–Landau kinetics has been discounted for processes involving solute conservation. The following argument makes the essential contrary point. Paraphrasing Cahn and Hilliard [10, 24], we are led to a one-dimensional theory with Ginzburg–Landau mean field thermodynamics and constant Bragg–

Williams coefficients. In this we incorporate n_v atoms/unit volume, the lattice parameter a and Cahn's gradient energy coefficient κ estimated as $2n_v kT_c a^2$ for bcc with

$$\frac{\mathrm{d}^2 f}{\mathrm{d}c^2} = 4n_v k(T - T_c). \tag{1}$$

In the absence of coherency strain incorporating a binomial expansion of the ideal entropy with c normalized for symmetry about $1/2$ we obtain, following Cahn and Hilliard [10, 24]

$$\frac{\partial c}{\partial t} = M_C a^2 \nabla^2 \frac{\delta F}{\delta c} = M_C a^2 \left[4n_v k(T - T_c) \left[\frac{\partial^2 c}{\partial x^2} \left\{ 1 - 3\left(\frac{c}{c_{eq}} \right)^2 \right\} \right.\right.$$
$$\left.\left. -6\frac{c}{c_{eq}^2} \left(\frac{\partial c}{\partial x} \right)^2 \right] - 2\kappa \frac{\partial^4 c}{\partial x^4} \right] \qquad M_C > 0. \tag{2}$$

The corresponding G–L reaction–diffusion formulation with Prigogine reaction kinetics [2], from which (2) can be derived by double differentiation, is

$$\frac{\partial c}{\partial t} = -M_G \frac{\delta F}{\delta c} = M_G \left[4n_v k(T_c - T)c \left\{ 1 - \left(\frac{c}{c_{eq}} \right)^2 \right\} + 2\kappa \frac{\partial^2 c}{\partial x^2} \right] \qquad M_G > 0. \tag{3}$$

M_C has been normalized such that both M have the units of frequency per unit energy. Solute conservation has been imposed on equation (2) requiring all terms on the right to be products of an even derivative and a constant or even function. From this requirement equation (3) is also conservative, but requires inclusion of a Lagrange multiplier for off-symmetry cases [25].

Clearly, differentiating the RHS of (3) twice with a view to assuring conservation of global c in equation (2) introduces a kind of circularity if not an overdetermination. Larché and Cahn [26] in their discussion of the Ginzburg–Landau variational derivative containing a coherency strain energy term actually included this solute-conserving multiplier, unaware that it vanishes at alloy symmetry. They then explained how to evaluate it, but without actually doing so, and proceeded to differentiate it away so as to reach their fourth order Fick-type diffusion equation. A unique fastest growing wavelength and singular behaviour for amplitudes exceeding the spinodes (equation (2)), neither of which are unequivocally observed, appear to be a consequence.

Evidently equation (3) is smoothly integrable from a quench up to heterogeneous equilibrium where $c = c_{eq} \simeq \sqrt{1 - T/T_c}/2$ while equation (1) is restricted to $<$ spinodal amplitudes ($c \sim c_{eq}/\sqrt{3}$) unless a stochastic modification is incorporated [24]. This distinction reserves steady state solutions to the TDGL (equation (3)), which pertains to the aforementioned lamellar products at near equilibrium.

4. A semi-empirical treatment of coherency strain

The local dilatations which occur in equilibrium alloys evaluated using Vegard's law act to uniquely define the solution thermodynamics expressed through regular solution pairing energies. With specific application to Au–Ni, Friedel [4] found that the Hume-Rothery size rule can be quantified through evaluating the respective contributions to the homogeneous free energy density and recognizing that the limiting extreme of solubility for a miscibility gap will be expressed when T_c approaches the solidus temperature, T_m. In Friedel's calculation of the Vegard's law effect upon clustering, where this is assumed to be the *dominant source of repulsion* between large atoms and small ones, he found for Au–Ni with $\xi = \mathrm{d}a/a_0\,\mathrm{d}c$ that

$$4\xi^2 \mu \leqslant 2n_v kT_m \tag{4}$$

where μ is the shear modulus. The largest solid state ξ is given by the equality which implies, in agreement with experiment, that ξ corresponds to $r_{Au} \sim 1.15 r_{Ni}$. This is the Hume-Rothery

maximum for predicting a full solubility range above T_c. But T_c is almost equal to T_m so Au–Ni identifies a special marginal case of equation (3) upon substitution of the equality in equation (4). One outcome is that $4\xi^2\mu$ can be expressed as the equivalent of a directed pairing energy ω ($2kT_c = Z\omega$)

$$n_v\omega \simeq 4\xi^2\mu/Z. \tag{5}$$

Consequently, we can deduce from (3), (4) and (5) that in three dimensions the incipient diffuse wall between the Au-rich and Ni-rich dendrites previously conceived in relation to figure 3 is described by

$$\frac{1}{M_G}\frac{\partial c}{\partial t} = \left\{2Zn_v\omega(1 - T/T_c)\left[1 - \left(\frac{c}{c_{eq}}\right)^2\right]c + Zn_x\omega a^2\nabla^2 c\right\} \tag{6}$$

where the strain effect appears consistently in a repulsive role as dominant in the uphill bulk reaction and attractive in the downhill diffusion-like term. As noted before, the interesting and highly consistent consequence of this approximate construction is that the stress field associated with the emerging coherency strain must be deemed identical to that which would be deduced from the incipient surface tension and the internal 'surface' saddle point array defined by the interleaved dendrite walls, thus reemphasizing the chemical nature of Vegard's law strain.

At root this equivalence obtains for the irreversible thermodynamic reason that there exists at least 3 kT of fluctuation free energy per atom in comparison with the total pairing energy $4kT_c$ per atom so the quasi-static constraints in Cahn–Hilliard theory [10, 24, 26] are overridden in such a way that the distinction between elastic and chemical energy emphasized by Cook and de Fontaine [9] becomes untenable.

If we analyse the states of inequality in equation (4) and suppose that the total pairing effect originally envisioned in equation (3) can be greater than the strain effect [1] we can prorate the coefficient of the uphill and downhill terms on the right to accommodate a mixed mechanism [4], *viz*., with the substitution of $n_v\omega$ in (6), we have the common coefficient

$$\left[8\xi^2\mu + 4n_vk\left(T_c - 2\frac{\xi^2\mu}{n_vk}\right)\right]. \tag{7}$$

Keep in mind that T_c is in all cases empirical so that the Hume-Rothery limit can be reached by combination of pairing mechanisms, or if one or the other or both are weakened, T_c must be decreased relative to T_m and the temperature range of full solubility increased. All of this of course holds within the regular solution approximation.

Proceeding as usual via a sinusoidal solution of equation (3) at low amplitude and generalizing from the foregoing bcc construction, we obtain the estimated critical wavelength with z the areal coordination number,

$$\lambda_c = 2\pi a\sqrt{\frac{z}{Z}\frac{1}{(1 - T/T_c)}} \tag{8}$$

independent of mechanism, which gives the right magnitude to accord with all of the observations in Au–Ni since 1961. Missing from this analysis is nature's rule for selecting the most probable initial wavelength. Hillert gives a heuristic argument in favour of $3\lambda_c$ [31], which is a plausible result for a process which transforms coherently to a lamellar 'pearlite' [15].

The most widely accepted treatment of coherency strain in stochastically reactive crystalline solids was due to Cahn [10] and Hilliard [24] and later amplified by Larché and Cahn [26]. It ignores the aforementioned pairing solution effects of strain while implying a drastic lowering of T_c, both results which countermand the natural atom repulsion effect of positive ξ in ω and which have never been unequivocally established experimentally [27].

In Cahn–Hilliard theory for Au–Ni, the trailing downhill term of $-\delta F/\delta c$ dominated by Vegard's law strain does not exist and is replaced on the RHS of equation (2) by $-2\xi^2 Y$, where the equilibrium state accessible ($\partial c/\partial t = 0$) implies the heterogeneous temperature relation

$$T = T_c(1 - \xi^2 Y/4\xi\mu) \tag{9}$$

which is a constant on the right and therefore physically meaningless. It appears that this marginal anomaly is ultimately a consequence of improperly entering a heterogeneity effect in the form of a wavelength-independent homogeneous one, which is to say, violating the considerable currency in physics of Taylor–Landau analyticity.

A remark concerning loss of coherency as recorded in figures 3, 4 and 6 is in order. This pertains to the creation of dislocation arrays, which is the precursor to lamellar decomposition at a sharp (<10 nm thick) conducting front. As a matter of consistency and completeness the latter process connects directly to the disposition of the initiating coherency strain because lamellar decomposition requires more-or-less complete, near reversible prior reversion to a locally strained uniform composition within a rich, highly conducting, high entropy plasma of dislocations and vacancies. This reversion can only be effected through the downhill gradient term as the unique source of stored free energy and the vehicle for substantial recovery of at least part of the initial bulk supersaturation which is required to drive the lamellar successor. Simultaneous formation of Cottrell atmospheres may also be involved.

5. Nucleation-free crystal boundaries

Underwood was prescient in naming the lamellar structure in Au–Ni 'pearlite' for it shares many elements of the Fe–C eutectoid alloys within theory and observation. On the theoretical side, the two-dimensional G–L equation possesses lamellar solutions incorporating diffuse triple points and connecting near equilibrium boundaries [19]. Furthermore, conventional Fe–C–X pearlites which form by phase boundary diffusion are commonly nodular with crystallographic templating at austenite grain boundaries as well as intragranularly. Some boundaries including twins are nucleation-free. There is a remarkably strong sense in which the TDGL equation offers both a static and dynamical impact, the contributions to the kinetics being separately applied in the eutectoid case.

The observations of nucleate-free or nucleation delayed boundaries in super-saturated Au–Ni alloys by Underwood at 673 K, Cahn at 993 K and Fisher and Embury [28] at 573 K for samples aged for lengthy times demand explanations. Although none of these examples are direct evidence, substantial modulated decomposition contacting such boundaries must have occurred in every case. Figure 13 is reproduced from Fisher and Embury. The upper boundary is evidently part of a twin since Underwood and Cahn and Hegel observed that these are inactive as nucleation sites. The lower one possesses curvature and is nucleation active on one side as often observed by Cahn and Hegel in Fe–C–X and by Underwood in Au–Ni. Deducing from the ⟨100⟩ dendrite in figure 11 that the elongated structure in figure 13 is equivalent we can specify that the short lived lamellar structure emerging above the entire boundary length shares this directionality and must have accordingly been templated by prior modulations, ignoring any bias originating with boundary structure. We observed this phenomenon at 773 K but did not succeed in capturing it on film. In this comparison with eutectoids, we find that it even has relevance to bainites (figures 11 and 13) and to the form of the time–temperature-transformation curve [15].

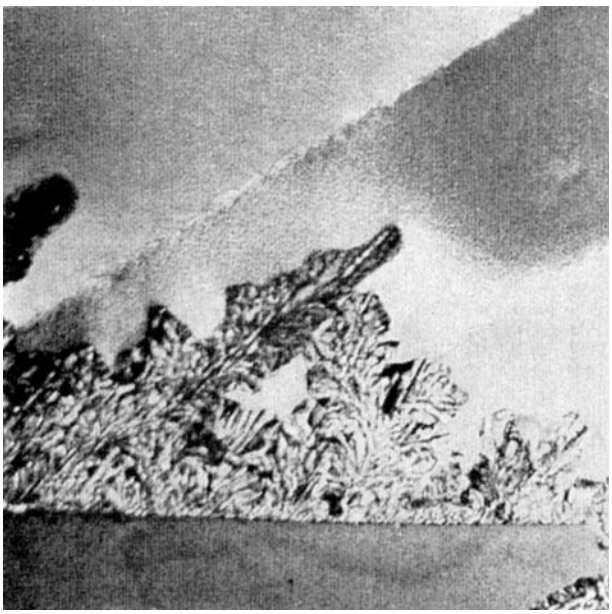

Figure 13. Nucleation of Au–Ni lamellar structure at a grain boundary growing in the ⟨100⟩ direction thereby indicating nucleation templating on spinodal modulations (see explanation in text). After Fisher and Embury [28].

6. Discussion

In 1971 Cook and de Fontaine [9] recognized the paradoxical relationship of Cahn and Friedel–Eshelby treatments of coherency strain in spinodal decomposition and attempted a partial resolution in terms of Khachaturyan's *static* concentration wave or harmonic analysis [3], even though it is unlikely that a theory requiring periodic boundary conditions has relevance to an autonomous process [5]. Larché and Cahn make no reference to this important contribution in their 1992 recapitulation of the standard strain-energy-dependent theory [15]. Very recently, Cahn reported a previously unpublished Au–Ni decomposition experiment at 993 K [29] exhibiting copious intragranular nodules, presumably of the faceted form observed by Underwood up to 973 K. We have to interpret this as strongly favouring the strain-inclusive solution theory of Friedel and Eshelby [4, 30]. Cahn has further emphasized that within his Fick-type diffusion model the growth of fluctuations in a supersaturated solution is excluded [10], so a solution must be framed in terms of a smooth or long wavelength initial value perturbation, and by example this was demonstrated by Hillert in his original discrete representation [31] of what became Cahn phenomenological theory. In contradiction, when the ternary extension of Cahn theory is addressed it is easily shown that the required capability of mounting an initial value problem is impossible to formulate because the non-commuting coefficient matrices of the second and fourth derivatives cannot be simultaneously brought to the diagonal [32]. Secondly, Larché and Cahn [26] adopt the fourth order equation with the usual coherency strain correction yielding the following paradox: below T_c this is supposed to have no effect on the downhill diffusion term, but instead acts to oppose and even to suppress completely the so-called uphill diffusion process. On the other hand when applied above T_c, as for example in [26] and in phase field applications, it acts to maximize the rate of downhill diffusion. Free of such conflict, Ginzburg–Landau theory generates clustering and reversion for

$T < T_c$, by *definition* discarding the reaction term at local equilibrium outside the miscibility gap, the gradient term now being discontinuously modified for gradient *free* energy so as to accommodate ordinary diffusion.

In seeking a deeper phenomenological understanding, we have been led to reexamine the seminal Ginzburg–Landau treatment of superconductivity [6], where the absolute value of the scalar ψ function can be taken to map to the scalar concentration c and the vector potential to a vector component of the displacement tensor u (or magnetic self-field to self-strain [24]). Besides the two gradient squared terms in the energy density there appears a positive cross-term predicated upon field theory gauge invariance which by mapping includes a term $\sim(u_c)^2$, and since $u \sim \xi c$ this ends up as a quartic in c. This increases the magnitude of the quartic term in the Taylor expansion of the thermodynamics involved in equations (3) and (6) which would normally terminate the modulation amplitudes at equilibrium values. The new term would accordingly act to reduce the attainable amplitudes of the modulations in proportion to ξ^2 but would have no effect upon the early stage of the reaction. Such behaviour might be regarded as a reasonable compromise between the Cahn–Hilliard and Ginzburg–Landau formulations.

In 1994 Goryachev [25] challenged the validity of the Cahn–Hilliard equation on the grounds that a Fickian conservative diffusion flux formulation from linear irreversible thermodynamics cannot rationally be applied to a chemical potential form like $\delta F/\delta c$ which contains gradient forms. He also cited certain anomalies in the reciprocal space solutions which are removed using a G–L formulation provided a Lagrange multiplier for solute conservation is appropriately entered. We have recognized that in real space these irrationalities are represented by the absence of a universally defined cut-off wavelength at the Hume-Rothery margin (cf equation (10)), global sample boundary conditions which are inappropriate to a completely autonomous system [5], the impossibility of framing an initial value problem within the ternary generalization [32] and an untenable analytic continuation to $T > T_c$ which violates the second law in the ideal solution limit (equation (2)). In tandem with these theoretical anomalies a wide range of experiments and discrete computational models have failed to find or predict unequivocally the unique fastest growing wavelength at early times implied by equation (2) [27] or the barrier to continuous growth of amplitudes beyond the spinodes. The present contribution adds to this the failure of Cahn–Hilliard theory to correctly generate the effects of coherency strain in the conventional down-quench autonomous experiment in Au–Ni. This is in contrast to the semi-quantitative success of presently modified TDGL theory in encompassing the dominant observations.

It is worth noting that Cahn–Hilliard theory as modified by Cook and de Fontaine [9] could have application to reversion experiments [24]. Yang [33] has illustrated such an application by reversion of epitaxial [111] Au–Ni films of short wavelengths where the boundary and initial conditions are appropriate to a diffusion model with an externally imposed strain field. Furthermore, in the more usual down-quench, the Hillert-Cahn–Hilliard qualitative conclusion as to the existence of diffuse phase boundaries in the double-well context stands as a singular achievement of 20th century chemical physics [29].

The simplest summary of our theoretical viewpoint is to recognize that a miscibility gap implies repulsion between unlike atoms in which the Hume-Rothery size effect due to the Pauli principle can represent the dominant chemical solution effect. The ensuing clustering reaction after a quench consists of a near homogeneous fluctuation-induced local repulsive separation, creating incipient surface in which the *responsive* gradient energy acts diffusively to flatten the profiles, and these profiles are subject in turn to further fluctuation amplitude accumulation. Positive free energy fluctuations of order kT per atom per degree of freedom encompassing the free-energy density function automatically surmount any implied barrier due to curvature or relaxed atom misfit thereby favouring the TDGL over any form of the C–H equation.

For historical reasons, we have continued to employ the term 'spinodal decomposition'. However, for scientific precision it must be emphasized that the spinodes do not enter the Ginzburg–Landau formulation in any empirically significant way.

These experiments in Au–Ni and fair closure with theories originating with Hume-Rothery's discoveries should serve as the basis for planning more realistic discrete models and continuous phenomenological formulations which are capable of incorporating explicit concentration dependences and the complicating presence of interactions between decomposition and local long range order.

Acknowledgments

The authors wish to thank Jim Garrett, Fred Pearson and Aleksandra Perovic for technical assistance.

References

[1] Pearson W B 1958 *Handbook of Lattice Spacings and Structures of Metals* (London: Pergamon) pp 20, 53
[2] Prigogine I 1955 *Introduction to Thermodynamics of Irreversible Processes* (Springfield, IL: Thomas) pp 40 ff
[3] Khachaturyan A G 1983 *Theory of Structure Transformations in Solids* (New York: Wiley) pp 97, 493 ff
[4] Friedel J 1954 *Adv. Phys.* **3** 446
[5] Penrose O and Fife P C 1980 *Physica* D **43** 44
[6] Ginzburg V L and Landau L D 1950 *Sov. Phys.–JETP* **20** 1064
[7] Landau L D and Khalatnikov C M 1954 *Akad. Nauk* **96** 469
[8] Averbach B L, Flinn P L and Cohen M 1954 *Acta Metall.* **2** 92
[9] Cook H E and De Fontaine D 1971 *Acta Metall.* **19** 607
[10] Cahn J W 1961 *Acta Metall.* **9** 795
[11] Pearson W B 1954 *Nature* **173** 364
[12] Abadias G, Marty A and Gilles B 1998 *Acta Metall.* **46** 4603
[13] Sinclair R, Gronsky R and Thomas G 1976 *Acta Metall.* **24** 789
[14] Köster W and Dannöhl W 1936 *Z. Metallk.* **28** 248
[15] Underwood E E 1954 *PhD Dissertation* MIT
[16] Gust W, Predel B and Nguyen Tat T 1976 *Z. Metallk.* **67** 110
[17] Purdy G R 1991 *Materials Science and Technology* vol 5, ed R W Cahn, P Haasen and E J Kramer (Weinheim: VCH) p 305
[18] Kirkaldy J S 1999 *Scr. Mater.* **39** 611
[19] Kirkaldy J S 2000 *Nucleation and Growth Processes in Materials* vol 44, ed A Gonis, P Turché and A Ardell, p 153
[20] Krznowski J E and Allen S M 1984 *Surf. Sci.* **44** 153
[21] Chen L-Q and Khachaturyan A G 1991 *Acta Metall. Mater.* **39** 2533
[22] Maugis P 1996 *Phys. Rev.* B **53** 5276.
[23] Noether S E 1918 *Nach. Ges. Wiss. Göttingen* **2** 235
[24] Hilliard J E 1970 *Phase Transformations* (Metals Park, OH: ASM)
[25] Goryachev S B 1994 *Phys. Rev. Lett.* **72** 1850
[26] Larché F C and Cahn J W 1992 *Acta Metall. Mater.* **40** 525
[27] Binder K 1991 *Materials Science and Technology* vol 5, ed R W Cahn, P Haasen and E J Kramer (Weinheim: VCH) p 405
[28] Fisher R M and Embury J D 1964 *3rd Eur. Regional Conf. on Electron Microscopy* (Prague: Publishing House of the Czechoslovak Academy of Sciences)
[29] Carter W C and Johnson W C (eds) 1998 *The Selected Works of J W Cahn* (Warrendale, PA: TMS)
[30] Eshelby J D 1956 *Adv. Solid State Phys.* **3** 79
[31] Hillert M 1961 *Acta Metall.* **9** 525
[32] Kirkaldy J S 2000 *J. Mater. Sci.* **35** 1177
[33] Yang W M-C 1971 *PhD Dissertation* Northwestern University